processes

MDPI

*Article*

# A Fractional Creep Model for Deep Coal Based on Conformable Derivative Considering Thermo-Mechanical Damage

**Lei Zhang [1,*], Chunwang Zhang [2,*], Ke Hu [3], Senlin Xie [4], Wenhao Jia [5] and Lei Song [4]**

[1] College of Safety and Emergency Management Engineering, Taiyuan University of Technology, Taiyuan 030024, China
[2] Center of Shanxi Engineering Research for Coal Mine Intelligent Equipment, Taiyuan University of Technology, Taiyuan 030024, China
[3] Civil and Environmental Engineering Department, University of Alberta, Edmonton, AB T6G 2H5, Canada; kh10@ualberta.ca
[4] School of Energy and Mining Engineering, China University of Mining and Technology-Beijing, Beijing 100083, China; xslcomeon@163.com (S.X.); songlei_leo@126.com (L.S.)
[5] School of Mechanics and Civil Engineering, China University of Mining and Technology-Beijing, Beijing 100083, China; jiawenhao95@163.com
* Correspondence: e_zhanglei@163.com (L.Z.); zhangchunwang@tyut.edu.cn (C.Z.)

**Abstract:** In deep high-geostress and high-temperature environments, understanding the creep deformation of deep coal is of great significance for effectively controlling coal deformation and improving gas control efficiency. In this paper, the Abel dashpot is defined based on the conformable derivative, and a damage variable is introduced into the conformable derivative order, thereby constructing a damaged Abel dashpot. Combining the Weibull distribution and the Drucker–Prager yield criterion, the thermo-mechanical coupling damage variable is defined, and the coupling damage variable is introduced into the damaged Abel dashpot to establish a thermo-mechanical coupling damaged Abel dashpot. Based on the traditional framework of the Burgers creep model, a three-dimensional fractional creep model of deep coal considering the influence of thermo-mechanical coupling damage is proposed. Experimental data on coal creep under different temperatures and stress conditions are utilized to validate the effectiveness and applicability of the proposed three-dimensional fractional creep model and to determine the model parameters. A comparison between experimental data and model results reveals that the creep model effectively characterizes the time-dependent deformation of coal samples under varying temperature and stress influences. Additionally, an in-depth analysis is carried out on the influence mechanism of key parameters in the creep model, particularly focusing on the effects of stress levels and temperature on creep deformation.

**Keywords:** deep coal; fractional creep model; thermo-mechanical damage; conformable derivative



**Citation:** Zhang, L.; Zhang, C.; Hu, K.; Xie, S.; Jia, W.; Song, L. A Fractional Creep Model for Deep Coal Based on Conformable Derivative Considering Thermo-Mechanical Damage. *Processes* **2024**, *12*, 1121. https://doi.org/10.3390/pr12061121

Academic Editor: Carlos Sierra Fernández

Received: 1 April 2024
Revised: 27 May 2024
Accepted: 27 May 2024
Published: 29 May 2024



## 1. Introduction

In recent years, extensive exploitation of shallow coal resources has led to a progressive decline in their reserves, prompting a shift towards deeper coal mining. However, the geological conditions in deep mines, characterized by "three highs" (high geostress, high temperature, and high seepage pressure) [1], pose significant challenges, with frequent occurrences of mining disasters. Moreover, the mechanisms underlying these disasters are notably intricate compared to those in shallow mines. Specifically, in deep high-gas mines, effective gas management measures are crucial to prevent coal and gas outburst disasters by reducing gas pressure and concentration to meet safety production standards [2]. With the extension of gas control periods, the creep deformation and visco-elastoplastic deformation of coal under long-term loading exert significant effects on coal seam roadways and gas extraction boreholes. This results in the inward convergence of roadways and the collapse or closure of gas extraction boreholes, consequently affecting roadway stability and gas control

efficiency [3]. Hence, thorough research into creep deformation in deep environments is crucial for gas control and coal mining.

As the development and mining timescales of deep coal mines extend, rheological phenomena become increasingly prominent within deep coal seams, impacting both gas control and coal resource extraction [4,5]. In order to delve deeper into the creep deformation of coal, researchers have conducted extensive work in this area [6–8]. Cao and Xian [9] conducted experimental research on the uniaxial and triaxial creep deformation of coal and analyzed the creep damage evolution, investigating the influencing factors. Wang et al. [10] obtained creep curves under different external pressure and gas pressure conditions and conducted in-depth analyses of the influencing mechanisms of creep deformation. Wang et al. [11] discovered that when outburst coal was subjected to low-stress conditions, it exhibited attenuated creep characteristics. However, when the pressure on the outburst coal exceeded its long-term strength, it displayed a non-attenuated creep trend. Yin et al. [12] studied both traditional triaxial creep curves and creep curves under unloading pressure, obtaining insights into the viscoelastic deformation under mining stress.

Through the aforementioned experimental research, researchers have gained a profound understanding of coal rheology, especially its creep characteristics, accumulating valuable experience for the study of theoretical models. Wang et al. [13], aiming to determine the creep law of gas-containing coal, proposed a triaxial creep constitutive model based on the Nishihara model. This model effectively describes the creep deformation characteristics of gas-containing coal under varying loads. Qi et al. [14], by linking a nonlinear strain-triggering element with the Nishihara model, proposed an improved model. They derived the constitutive equation for three-dimensional creep under constant stress conditions and validated the creep model using experimental data. This model accurately describes the creep characteristics during the accelerated creep stage of sandstone. Cai et al. [15] established a visco-elastoplastic constitutive model that conforms to the deformation patterns of low-rank coal. This model incorporates hardening and damage functions, enabling it to effectively characterize the deformation behavior of low-rank coal under various load levels. Meanwhile, Qu [16] improved the Burgers model by serially connecting it with a nonlinear visco-elastoplastic body, deriving a triaxial creep constitutive model. The accuracy of the model was verified using experimental data, demonstrating its ability to depict the deformation evolution during the accelerated creep stage of coal.

Based on the research into creep models and other nonlinear models mentioned above, the description of nonlinear problems has become a research hotspot. As research progresses, fractional derivatives have emerged as effective tools for studying nonlinear problems and have been introduced into theoretical constitutive models to characterize viscoelastic and viscoplastic deformations [17,18].

Zhou et al. [19] developed a new Abel dashpot based on fractional derivatives. They utilized the fractional Abel dashpot to replace the classic dashpot in the Nishihara model, establishing a fractional rheological model capable of describing the creep deformation of salt rock, particularly the tertiary creep stage. Kang et al. [20] introduced a nonlinear creep model incorporating a fractional Scott–Blair element to describe the creep process of coal, and included a damage factor to characterize the tertiary creep stage. Wang et al. [21] proposed a creep constitutive equation under triaxial stress conditions, including volumetric creep. The creep constitutive equation was validated and its parameters were determined using creep curves of deep coal, demonstrating that the creep constitutive equation can effectively depict the entire creep process.

It should be noted that high temperature also affects the creep behavior characteristics of coal and rock [22]. Therefore, research on creep models under coupled conditions of high temperature and high geostress in deep areas has attracted widespread attention [23,24]. Zuo et al. [25] considered the impact of temperature on mechanical components from a theoretical model perspective. They established a creep model with thermo-mechanical coupling effects and analyzed the creep deformation results of the model in conjunction with experimental data. Xi et al. [26] developed a mechanical model of thermo-visco-

elastoplastic elements and proposed a creep model incorporating thermo-mechanical coupling effects based on the Nishihara model, and validated the creep model using experimental curves under different temperature and load levels. Based on the Weibull distribution and the Lemaitre equivalent strain principle, Xu and Karakus [27] established a damage model for granite with thermo-mechanical coupling effects and analyzed the evolution process of thermal damage and mechanical damage. Research on the creep behavior with the aforementioned thermo-mechanical coupling effects mainly focuses on constructing integer derivative creep models, with few reports on fractional derivative creep models. Moreover, existing studies often emphasize the degradation of mechanical parameters, with limited utilization of changes in fractional derivative order to reflect the creep deformation behavior under thermal-mechanical coupling.

In order to investigate the creep behavior and evolutionary mechanism of coal under high-temperature and high-geostress conditions, this paper establishes a fractional derivative creep model from a theoretical standpoint. The study delves into the creep deformation of coal under varying temperatures and stress conditions. By defining the Abel dashpot through the conformable derivative and integrating the damage variable into the conformable derivative order, a damaged Abel dashpot is constructed. Furthermore, the thermo-mechanical coupling damage variable is defined based on the Weibull distribution and the Drucker–Prager yield criterion. The coupling damage variable is then incorporated into the damaged Abel dashpot to establish a thermo-mechanical coupling damage Abel dashpot. Drawing upon the traditional framework of the Burgers creep model, the study incorporates the Abel dashpot and the thermo-mechanical coupling damage Abel dashpot, proposing a triaxial fractional creep model that accounts for the influence of thermo-mechanical coupling damage. The effectiveness and applicability of the proposed fractional creep model are validated using experimental creep data obtained under various temperature and stress conditions. Model parameters are refined through fitting procedures. Additionally, the influence mechanism of the critical parameters of the fractional creep model is deeply analyzed.

## 2. Definition of the Damaged Abel Dashpot and Damage Variable

### 2.1. The Damaged Abel Dashpot

Creep deformation can be considered as a combination of elastic deformation, viscoelastic deformation, and viscoplastic deformation, with viscoelastic deformation being the primary factor controlling the magnitude of long-term creep deformation. In order to analyze the evolution of viscoelastic deformation from a theoretical perspective, researchers have constructed various forms of dashpot elements to explain the mechanism of viscoelastic deformation [18,19]. The most commonly used dashpot element is the Newton dashpot, and classical models such as the Nishihara model, and Burgers model all adopt the Newton dashpot to describe viscoelastic deformation. The stress–strain relationship equation of the Newton dashpot (Figure 1a) is as follows:

$$\sigma = \eta \frac{d\varepsilon(t)}{dt} \tag{1}$$

where $\eta$ is the viscosity coefficient, GPa·h.

As research delves deeper, fractional derivatives have been introduced as effective tools for describing nonlinear deformation in the expression of viscoelastic elements [19,20]. The varying order of fractional derivatives, ranging between 0 and 1, grants them enhanced flexibility in capturing viscoelastic deformation accurately. Drawing an analogy with the classic Newton dashpot, this paper presents the stress–strain relationship equation of the Abel dashpot (Figure 1b) based on the conformable derivative [28,29]:

$$\sigma = \eta T_\gamma[\varepsilon(t)] \quad (0 < \gamma \leq 1) \tag{2}$$

Based on the conversion relation between of first derivative and conformable derivative [28,30]:

$$T_\gamma[\varepsilon(t)] = t^{1-\gamma}\frac{d\varepsilon(t)}{dt} \tag{3}$$

when the conformable derivative order $\gamma$ equals 1, the conformable derivative degrades to the standard first derivative.

Substituting Equation (3) into Equation (2) yields the following relationship [28,29]:

$$\sigma = \eta\frac{d\varepsilon(t)}{dt}t^{1-\gamma} \quad (0 < \gamma \leq 1) \tag{4}$$

By integrating Equation (4) with the initial condition $\varepsilon(0) = 0$, the stress–strain solution for the Abel dashpot under constant stress is as follows:

$$\varepsilon(t) = \frac{\sigma}{\eta}\cdot\frac{t^\gamma}{\gamma} \quad (0 < \gamma \leq 1) \tag{5}$$

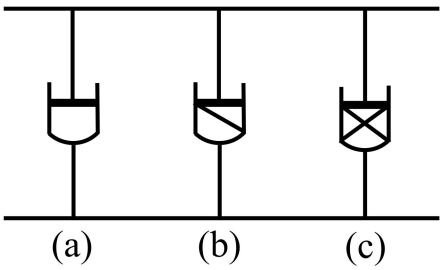


**Figure 1.** Dashpot element: (**a**) Newton dashpot, (**b**) Abel dashpot, (**c**) damaged Abel dashpot.

As depicted in Equation (5), the Abel dashpot proficiently characterizes time-dependent deformation during both the decaying creep and steady-state creep stages. Nevertheless, during the accelerated creep stage, creep deformation undergoes a substantial increase within a short period, rendering the conventional Abel dashpot insufficient for accurately depicting the time-dependent deformation in this phase. To address this limitation, numerous scholars have expanded the range of fractional order values and introduced damage variables to weaken mechanical parameters in creep constitutive model development. These efforts aim to precisely describe accelerated creep deformation.

Wu et al. [31] and Xue et al. [32] have each devised nonlinear dashpots based on fractional derivatives, extending the range of fractional order values beyond 1. The creep models derived from these approaches adeptly capture the accelerated creep phenomenon. Additionally, Zhou et al. [33] introduced damage variables into fractional order, creating a nonlinear damage dashpot. The creep model derived from this dashpot similarly accounts for accelerated creep behavior. Building upon these insights, this study integrates the conventional Abel dashpot expression with the definition of a conformable derivative, introducing a damage variable into the conformable derivative order. It constructs a damaged Abel dashpot (Figure 1c), whose constitutive relation is as follows:

$$\sigma = \eta\frac{d^{\gamma(1+D)}\varepsilon(t)}{dt^{\gamma(1+D)}} \quad (0 < \gamma \leq 1, 0 < D \leq 1) \tag{6}$$

By integrating Equation (6) with the initial condition $\varepsilon(0) = 0$, the stress–strain solution for the damaged Abel dashpot at constant stress is as follows:

$$\varepsilon(t) = \frac{\sigma}{\eta}\frac{t^{\gamma(1+D)}}{\gamma(1+D)} \quad (0 < \gamma \leq 1, 0 < D \leq 1) \tag{7}$$

It should be noted that when the damage variable is zero, the damaged Abel dashpot reverts to a conventional Abel dashpot. Assuming a stress of 30 MPa, a conformable derivative order of 0.9, and a viscosity coefficient of 5 GPa·h$^{\gamma}$, the time-dependent deformation evolution under different damage states can be derived using Equation (7). As depicted in Figure 2, for the conventional Abel dashpot when the damage variable is zero, the increase in time-dependent deformation over time is minimal. As the damage variable increases, the time-dependent deformation of the damaged Abel dashpot gradually amplifies. Moreover, the increased magnitude of deformation can be controlled by adjusting the value of the damage variable.

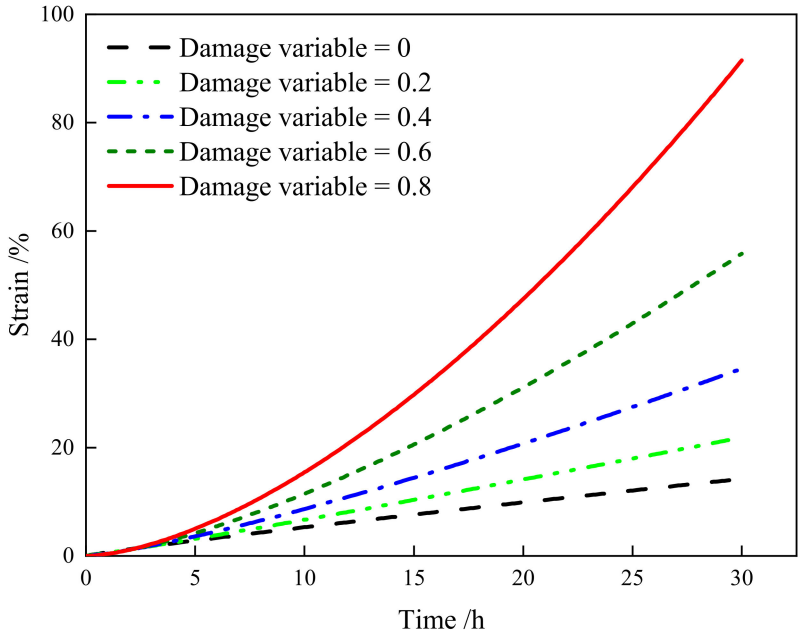


**Figure 2.** Time-dependent deformation curves of damaged Abel dashpot.

### *2.2. Thermo-Mechanical Coupling Damage Variable*

Under conditions of high temperature and high geostress, the deformation process of coal is accompanied by the accumulation of damage. This damage process is the result of thermo-mechanical coupling effects, and quantitatively describing the damage evolution has been a research hotspot. Considering the inhomogeneity of coal and rock materials and the randomness of internal defect distribution, the strength can be considered as a stochastic quantity influenced by certain internal variables. Due to the inhomogeneity of the structure and the randomness of coal microelement distribution, many micro-defects exist internally, resulting in varying strengths among microelements. Therefore, selecting an appropriate method to depict the distribution of coal microelement strength is crucial.

Based on the Weibull distribution, Hu et al. [34] constructed a creep constitutive relationship of salt rock under temperature-induced damage. Meanwhile, Ding et al. [35] utilized the Weibull distribution to model the evolution relationship between the number of acoustic emission events and loading time, thereby deriving the damage variable evolution equation. This equation effectively captures the temporal evolution of acoustic emission events. The Weibull distribution offers distinctive advantages in analyzing the statistical mechanics behavior of coal and rock masses.

When considering macroscopic damage of coal as continuous during the loading process, it can be assumed that coal microelements follow the generalized Hooke's law before failure and adhere to the Drucker–Prager yield criterion upon failure. Macroscopic damage is thus determined by the random failure of microelements, whose strength follows

a Weibull distribution [32,33]. The probability density corresponding to strength is denoted as $P(\varepsilon)$:

$$P(\varepsilon) = \begin{cases} \frac{m}{\varepsilon_0}\left(\frac{\varepsilon}{\varepsilon_0}\right)^{m-1} \exp\left[-\left(\frac{\varepsilon}{\varepsilon_0}\right)^{m}\right] & \varepsilon \geq 0 \\ 0 & \varepsilon < 0 \end{cases} \tag{8}$$

where $m$ represents the degree of inhomogeneity in the damage distribution of the microelement; $\varepsilon_0$ signifies a parameter characterizing the damage evolution; $\varepsilon$ denotes the axial strain of the microelement.

It should be noted that solely relying on axial strain $\varepsilon$ of microelement is insufficient to represent the influence of volumetric strain $\varepsilon_v$ under three-dimensional stress. Therefore, it is proposed to introduce the probability density distribution corresponding to volumetric strain $P(\varepsilon_v)$:

$$P(\varepsilon_v) = \frac{m}{\varepsilon_0}\left(\frac{\varepsilon_v}{\varepsilon_0}\right)^{m-1} \exp\left[-\left(\frac{\varepsilon_v}{\varepsilon_0}\right)^{m}\right] \tag{9}$$

Previous studies have shown that macroscopic damage is actually the probability integral of microelement strength distribution. Thus, the macroscopic damage variable $D$ can be obtained through the following form of probability integral:

$$D = \int_0^{\varepsilon_v} P(\varepsilon_v) d\varepsilon = 1 - \exp\left[-\left(\frac{\varepsilon_v}{\varepsilon_0}\right)^{m}\right] \tag{10}$$

Under thermo-mechanical coupling conditions, the actual stress state of a microelement is the result of the superposition of thermal expansion stress and external stress. The equivalent stress expression $\widetilde{\sigma_{ij}}$ under thermo-mechanical coupling conditions is obtained as follows:

$$\widetilde{\sigma_{ij}} = \sigma_{ij} + E\alpha_T \Delta T = E\widetilde{\varepsilon_{ij}} \tag{11}$$

where $E$ is the elastic modulus, GPa; $\widetilde{\varepsilon_{ij}}$ is the equivalent strain; $\alpha_T$ is the thermal expansion coefficient, $K^{-1}$; $\Delta T = T - T_0$ is the temperature increment, $T_0$ is the room temperature 25 °C.

Combining Equation (11), the macroscopic damage variable $D$ from Equation (10) can be transformed into a function of equivalent volumetric stress as follows:

$$D = 1 - \exp\left[-\left(\frac{\widetilde{\sigma_v}}{3K_0\varepsilon_0}\right)^{m}\right] \tag{12}$$

where the equivalent volumetric stress $\widetilde{\sigma_v} = \widetilde{\sigma_{11}} + \widetilde{\sigma_{22}} + \widetilde{\sigma_{33}}$; $K_0$ is the bulk modulus, GPa.

In Equation (12), the parameter $m$ is a key parameter of the Weibull distribution function, which is associated with the distribution of internal micro-defects and fracture networks. Previous studies have shown that this parameter is correlated with temperature [36], specifically as $m = a\Delta T + b$. Therefore, Equation (12) can be adjusted to the following form:

$$D = 1 - \exp\left[-\left(\frac{\widetilde{\sigma_v}}{3K_0\varepsilon_0}\right)^{a\Delta T+b}\right] \tag{13}$$

where $a$ and $b$ are temperature effect constants, which can be determined through fitting experimental data.

The traditional Nishihara model utilizes the Mises yield criterion to characterize the yielding, failure, and creep deformation of rocks. However, this yield criterion does not account for the influence of hydrostatic pressure and intermediate principal stress, leading to certain limitations in describing the yielding and failure behavior of coal. Therefore, this

paper adopts the Drucker–Prager yield criterion to depict the yielding and failure process of coal microelements [28,32], with the expression as follows:

$$\begin{cases} \widetilde{F} = \alpha \widetilde{I_1} + \sqrt{\widetilde{J_2}} - K, \\ \alpha = \frac{2\sin\varphi}{\sqrt{3}(3-\sin\varphi)}, K = \frac{6c\cos\varphi}{\sqrt{\sqrt{3}(3-\sin\varphi)}} \end{cases} \tag{14}$$

where $\alpha$ and $K$ are the parameters of Drucker–Prager yield criterion; $\widetilde{I_1}$ is the first invariant of the stress tensor; $J_2$ is the second invariant of the stress deviator; $\varphi$ is the internal friction angle, °; $c$ is the cohesion, MPa.

Since the first invariant of the stress tensor is equivalent to the equivalent volumetric stress, i.e., $\widetilde{I_1} = \widetilde{\sigma_v}$, the expression for the damage variable is as follows:

$$D = 1 - \exp\left[ -\left( \frac{\widetilde{I_1}}{3K_0\varepsilon_0} \right)^{a\Delta T + b} \right] \tag{15}$$

Under conventional triaxial compression conditions, where coal microelements experience stress boundaries $\widetilde{\sigma_{22}} = \widetilde{\sigma_{33}}$, the expression for the stress invariants is as follows:

$$\begin{cases} \widetilde{I_1} = \widetilde{\sigma_{11}} + 2\widetilde{\sigma_{33}} \\ \widetilde{J_2} = \frac{(\widetilde{\sigma_{11}} - \widetilde{\sigma_{33}})^2}{3} \end{cases} \tag{16}$$

According to the generalized Hooke's law, Equation (16) can be transformed into:

$$\begin{cases} \widetilde{I_1} = E\widetilde{\varepsilon_{11}} + 2\widetilde{\sigma_{33}}(1+\mu) \\ \widetilde{J_2} = \frac{\left[E\widetilde{\varepsilon_{11}} + \widetilde{\sigma_{33}}(2\mu-1)\right]^2}{3} \end{cases} \tag{17}$$

where $\mu$ is the Poisson's ratio.

Combining Equations (14), (15) and (17), the expression for the damage variable can established under the thermo-mechanical coupling effect:

$$D_{MT} = 1 - \exp\left[ -\left( \frac{6c\cos\varphi - \left[E\widetilde{\varepsilon_{11}} + \widetilde{\sigma_{33}}(2\mu-1)\right](3-\sin\varphi)}{6K_0\varepsilon_0\sin\varphi} \right)^{a\Delta T + b} \right] \tag{18}$$

Based on Equation (18), the evolution pattern of the damage variable is analyzed under different temperature and stress conditions. As shown in Figure 3, as the values of temperature and stress increase, the severity of damage intensifies. This trend aligns with the typical coal damage behavior in the thermo-mechanical coupling process.

For a specific temperature and stress environment, the damage extent to coal can be determined by Equation (18). However, it cannot describe the continuous evolution of damage over time during the creep process. In order to present the time-dependent characteristics of the damage variable, we introduce the concept of time-dependent damage variable $D_t$ defined by a negative exponential function [19]:

$$D_t = 1 - \exp(-\omega t) \tag{19}$$

where $\omega$ is the time effect parameter, $h^{-1}$.

Based on the coupled damage combination form shown in Equation (20), we define the thermo-mechanical coupling damage variable $D_{MT}(t)$ with time-dependent characteristics during the creep process as shown in Equation (21):

$$D_{MT}(t) = D_{MT} + D_t - D_{MT}D_t \tag{20}$$

$$D_{MT}(t) = 1 - \exp\left[-\left(\frac{6c\cos\varphi - \left[E\widetilde{\varepsilon_{11}} + \widetilde{\sigma_{33}}(2\mu - 1)\right](3 - \sin\varphi)}{6K_0\varepsilon_0\sin\varphi}\right)^{a\Delta T + b} - \omega t\right] \tag{21}$$

According to Equation (21), the time-dependent evolution characteristics of the damage variable are analyzed under thermo-mechanical coupling conditions. As shown in Figure 4, with the increase in creep time, the damage variable gradually increases. Additionally, as the value of the time effect parameter increases, the thermo-mechanical coupling damage variable at the same creep time gradually rises.

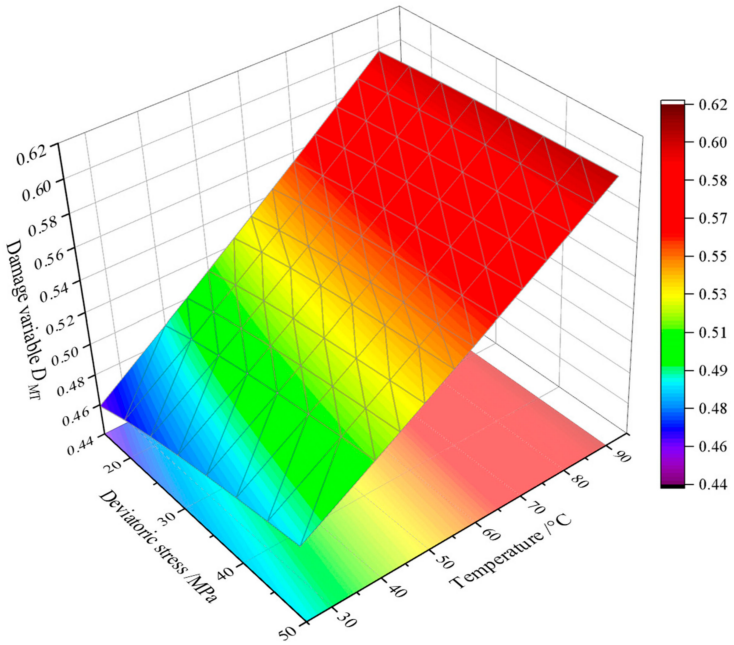


**Figure 3.** Schematic diagram of thermo-mechanical coupling damage surface.

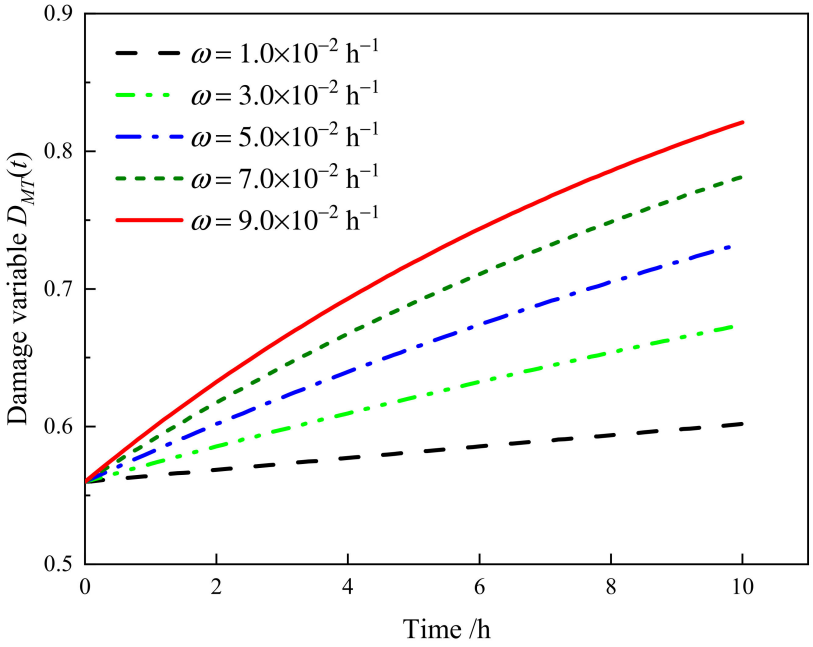


**Figure 4.** Damage variable curves with different time effect parameters.

## 3. Creep Model Development

### *3.1. One-Dimensional Creep Constitutive Model*

In this section, the traditional Newton dashpots in the Burgers model are replaced by an Abel dashpot and a damaged Abel dashpot considering the thermo-mechanical coupling damage effect. A fractional creep model considering thermo-mechanical coupling damage is established. This model includes a Maxwell body and a viscoplastic body, as depicted in Figure 5.

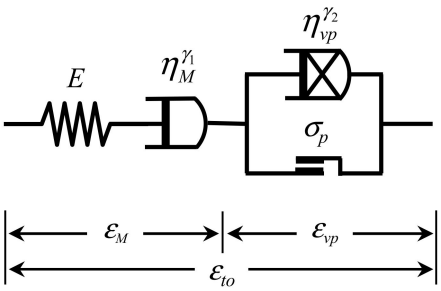


**Figure 5.** Fractional creep model considering thermo-mechanical coupling damage.

The total strain is given by:

$$\widetilde{\varepsilon_{to}} = \widetilde{\varepsilon_M} + \widetilde{\varepsilon_{vp}} \tag{22}$$

where $\widetilde{\varepsilon_M}$ is the strain of the Maxwell body, and $\widetilde{\varepsilon_{vp}}$ is the strain of the viscoplastic body.

(1) The stress–strain expression of the Hooke element in the Maxwell body is given by:

$$\widetilde{\varepsilon_M^e} = \frac{\widetilde{\sigma}}{E} \tag{23}$$

where $\widetilde{\varepsilon_M^e}$ represents the elastic strain of the Maxwell body.

The constitutive equation for the Abel dashpot, based on the definition of the conformable derivative, is given as follows:

$$\widetilde{\varepsilon_M^A} = \frac{\widetilde{\sigma}}{\eta_M^{\gamma_1}} \cdot \frac{t^{\gamma_1}}{\gamma_1} \tag{24}$$

where $\widetilde{\varepsilon_M^A}$ is the viscosity strain of the Maxwell body; $\gamma_1$ is the conformable derivative order; $\eta_M^{\gamma_1}$ is the viscosity coefficient, GPa·h$^{\gamma 1}$.

The strain of the Maxwell body is obtained by superimposing Equations (23) and (24), resulting in the following expression:

$$\widetilde{\varepsilon_M} = \widetilde{\varepsilon_M^e} + \widetilde{\varepsilon_M^A} = \frac{\widetilde{\sigma}}{E} + \frac{\widetilde{\sigma}}{\eta_M^{\gamma_1}} \cdot \frac{t^{\gamma_1}}{\gamma_1} \tag{25}$$

(2) For the viscoplastic body, the stress $\sigma_p$ of the fractional element is given by:

$$\sigma_p = \begin{cases} \widetilde{\sigma}, & \widetilde{\sigma} < \sigma_s \\ \sigma_s, & \widetilde{\sigma} \geq \sigma_s \end{cases} \tag{26}$$

where $\sigma_s$ represents the yield limit, MPa.

The total stress $\widetilde{\sigma}$ of the viscoplastic body is obtained by:

$$\widetilde{\sigma} = \sigma_d + \sigma_p \tag{27}$$

where $\sigma_d$ represents the stress of the damaged Abel dashpot, MPa.

If $\widetilde{\sigma} < \sigma_s$, integrating Equations (26) and (27), the stress of the damaged Abel dashpot $\sigma_d = 0$, i.e.,

$$\widetilde{\varepsilon_{vp}} = 0 \tag{28}$$

If $\widetilde{\sigma} \geq \sigma_s$, Equation (27) is rewritten as:

$$\widetilde{\sigma} = \eta_{vp}^{\gamma_2} T_{\gamma_2(1+D_{MT}(t))}\left[\widetilde{\varepsilon_{vp}}\right] + \sigma_s \tag{29}$$

where $\eta_{vp}^{\gamma_2}$ is the viscosity coefficient, GPa·h$^{\gamma 2}$; $\gamma_2$ is the conformable derivative order.

Equation (29) is deformed as:

$$T_{\gamma_2(1+D)}\left[\widetilde{\varepsilon_{vp}}\right] = \frac{\widetilde{\sigma} - \sigma_s}{\eta_{vp}^{\gamma_2}} \tag{30}$$

Combining the conformable derivative calculation rules and the initial condition $\widetilde{\varepsilon_{vp}} = 0$ when $t = 0$, a stress–strain solution Equation (31) can be obtained:

$$\widetilde{\varepsilon_{vp}} = \frac{\widetilde{\sigma} - \sigma_s}{\eta_{vp}^{\gamma_2}} \cdot \frac{t^{\gamma_2(1+D_{MT}(t))}}{\gamma_2(1+D_{MT}(t))} \tag{31}$$

The combination of Equations (28) and (31) leads to:

$$\widetilde{\varepsilon_{vp}} = \begin{cases} 0 & \widetilde{\sigma} < \sigma_s \\ \frac{\widetilde{\sigma}-\sigma_s}{\eta_{vp}^{\gamma_2}} \cdot \frac{t^{\gamma_2(1+D_{MT}(t))}}{\gamma_2(1+D_{MT}(t))} & \widetilde{\sigma} \geq \sigma_s \end{cases} \tag{32}$$

The strain of each mechanical element is superimposed, and the total creep strain of the fractional creep model considering thermo-mechanical coupling damage is given by:

$$\begin{cases} \widetilde{\varepsilon(t)} = \frac{\widetilde{\sigma}}{E} + \frac{\widetilde{\sigma}}{\eta_M^{\gamma_1}} \cdot \frac{t^{\gamma_1}}{\gamma_1} & \widetilde{\sigma} < \sigma_s \\ \widetilde{\varepsilon(t)} = \frac{\widetilde{\sigma}}{E} + \frac{\widetilde{\sigma}}{\eta_M^{\gamma_1}} \cdot \frac{t^{\gamma_1}}{\gamma_1} + \frac{\widetilde{\sigma}-\sigma_s}{\eta_{vp}^{\gamma_2}} \cdot \frac{t^{\gamma_2(1+D_{MT}(t))}}{\gamma_2(1+D_{MT}(t))} & \widetilde{\sigma} \geq \sigma_s \end{cases} \tag{33}$$

### *3.2. Triaxial Creep Constitutive Model*

The triaxial stress condition significantly influences the deformation and damage accumulation in deep coal. It is imperative to extend the one-dimensional creep model to the triaxial creep model to characterize the creep deformation and damage evolution behavior of coal. Therefore, this section proposes a fractional triaxial creep model under the thermo-mechanical coupling damage effect. Based on the principle of strain superposition, the total strain expression for the triaxial creep model is as follows:

$$\widetilde{\varepsilon_{ij}(t)} = \widetilde{\varepsilon_{ij}^{M}} + \widetilde{\varepsilon_{ij}^{vp}} \tag{34}$$

where $\widetilde{\varepsilon_{ij}(t)}$ is the total strain tensor; $\widetilde{\varepsilon_{ij}^{M}}$ is the strain tensor of the Maxwell body; $\widetilde{\varepsilon_{ij}^{vp}}$ is the strain tensor of viscoplastic body.

The three-dimensional stress–strain relationship of the elastic element based on the generalized Hooke's law can be expressed by:

$$\widetilde{\varepsilon_{ij}^{H}} = \frac{\widetilde{s_{ij}}}{2G_M} + \frac{\widetilde{\sigma_m}}{3K_M}\delta_{ij} \tag{35}$$

where $G_M$ and $K_M$ are the shear modulus and bulk modulus, respectively, GPa; $\widetilde{s_{ij}} = \widetilde{\sigma_{ij}} - \widetilde{\sigma_m}\delta_{ij}$ is the deviatoric stress tensor; $\widetilde{\sigma_m} = (\widetilde{\sigma_{11}} + \widetilde{\sigma_{22}} + \widetilde{\sigma_{33}})/3$ is the spherical stress tensor; and $\delta_{ij}$ is the Kronecker symbol.

According to Equation (24), the three-dimensional stress–strain expression of the Abel dashpot is as follows:

$$\widetilde{\varepsilon_{ij}^{A}} = \frac{\widetilde{s_{ij}}}{2\eta_M^{\gamma_1}} \cdot \frac{t^{\gamma_1}}{\gamma_1} \tag{36}$$

The three-dimensional stress–strain expression of the Maxwell body can be obtained by:

$$\widetilde{\varepsilon_{ij}^{ve}} = \frac{\widetilde{s_{ij}}}{2G_M} + \frac{\widetilde{\sigma_m}}{3K_M}\delta_{ij} + \frac{\widetilde{s_{ij}}}{2\eta_M^{\gamma_1}} \cdot \frac{t^{\gamma_1}}{\gamma_1} \tag{37}$$

Combining Equation (30) with the viscoplastic ansatz of the Perzyna type [37], the three-dimensional strain rate of the viscoplastic body is defined and expressed in the following form:

$$T^{\gamma_2(1+D_{MT}(t))}\left[\widetilde{\varepsilon_{ij}^{vp}}\right] = \frac{1}{2\eta_{vp}^{\gamma_2}}\left\langle \phi\left(\frac{\widetilde{F}}{F_0}\right)\right\rangle \frac{\partial \widetilde{F}}{\partial \sigma_{ij}} \tag{38}$$

where

$$\left\langle \phi\left(\frac{\widetilde{F}}{F_0}\right)\right\rangle = \begin{cases} 0 & (\widetilde{F} < 0) \\ \phi\left(\frac{\widetilde{F}}{F_0}\right) & (\widetilde{F} \geq 0) \end{cases} \tag{39}$$

where $\widetilde{F}$ and $F_0$ represent the yield function and the initial value; $\phi(\cdot)$ is the power function form.

Combining the conformable derivative calculation rules and the initial condition $\widetilde{\varepsilon_{ij}^{vp}} = 0$ when $t = 0$, the three-dimensional stress–strain expression of the viscoplastic body can be deduced by:

$$\widetilde{\varepsilon_{ij}^{vp}} = \frac{t^{\gamma_2(1+D_{MT}(t))}}{2\eta_{vp}^{\gamma_2}\gamma(1+D_{MT}(t))}\left\langle \phi\left(\frac{\widetilde{F}}{F_0}\right)\right\rangle \frac{\partial \widetilde{F}}{\partial \sigma_{ij}} \tag{40}$$

By analogy with the superposition principle of strain in the one-dimensional creep model, the strain expression of the triaxial creep model is as follows:

$$\begin{cases} \widetilde{\varepsilon_{ij}}(t) = \frac{\widetilde{s_{ij}}}{2G_M} + \frac{\widetilde{\sigma_m}}{3K_M}\delta_{ij} + \frac{\widetilde{s_{ij}}}{2\eta_M^{\gamma_1}} \cdot \frac{t^{\gamma_1}}{\gamma_1} & (\widetilde{F} < 0) \\ \widetilde{\varepsilon_{ij}}(t) = \frac{\widetilde{s_{ij}}}{2G_M} + \frac{\widetilde{\sigma_m}}{3K_M}\delta_{ij} + \frac{\widetilde{s_{ij}}}{2\eta_M^{\gamma_1}} \cdot \frac{t^{\gamma_1}}{\gamma_1} + \frac{t^{\gamma_2(1+D_{MT}(t))}}{2\eta_{vp}^{\gamma_2}\gamma_2(1+D_{MT}(t))}\left\langle \phi\left(\frac{\widetilde{F}}{F_0}\right)\right\rangle \frac{\partial \widetilde{F}}{\partial \sigma_{ij}} & (\widetilde{F} \geq 0). \end{cases} \tag{41}$$

Considering the confining pressure condition of the creep test, that is, $\widetilde{\sigma_2} = \widetilde{\sigma_3}$, then:

$$\begin{cases} \widetilde{s_{11}} = \widetilde{\sigma_{11}} - \widetilde{\sigma_m} = \frac{2}{3}(\widetilde{\sigma_{11}} - \widetilde{\sigma_{33}}), \widetilde{\sigma_m} = \frac{1}{3}(\widetilde{\sigma_{11}} + 2\widetilde{\sigma_{33}}) \\ \widetilde{I_1} = \widetilde{\sigma_{11}} + 2\widetilde{\sigma_{33}}, \sqrt{\widetilde{J_2}} = \frac{\widetilde{\sigma_{11}} - \widetilde{\sigma_{33}}}{\sqrt{3}} \end{cases} \tag{42}$$

Substituting Equations (39) and (42) into Equation (41), with the initial yield function $F_0 = 1$, the axial strain expression considering thermo-mechanical coupling damage can be obtained by:

$$\begin{cases} \tilde{\varepsilon}_{11}(t) = \frac{\tilde{\sigma}_{11}-\tilde{\sigma}_{33}}{3G_M} + \frac{\tilde{\sigma}_{11}+2\tilde{\sigma}_{33}}{9K_M} + \frac{\tilde{\sigma}_{11}-\tilde{\sigma}_{33}}{3\eta_M^{\gamma_1}} \cdot \frac{t^{\gamma_1}}{\gamma_1} & (\tilde{F} < 0) \\ \tilde{\varepsilon}_{11}(t) = \frac{\tilde{\sigma}_{11}-\tilde{\sigma}_{33}}{3G_M} + \frac{\tilde{\sigma}_{11}+2\tilde{\sigma}_{33}}{9K_M} + \frac{\tilde{\sigma}_{11}-\tilde{\sigma}_{33}}{3\eta_M^{\gamma_1}} \cdot \frac{t^{\gamma_1}}{\gamma_1} + \frac{t^{\gamma_2(1+D_{MT}(t))}}{2\eta_{vp}^{\gamma_2}\gamma_2(1+D_{MT}(t))} & (\tilde{F} \geq 0) \\ \quad \cdot \left(\alpha + \frac{\sqrt{3}}{3}\right) \cdot \left(\alpha\left(\tilde{\sigma}_{11} + 2\tilde{\sigma}_{33}\right) + \frac{\tilde{\sigma}_{11}-\tilde{\sigma}_{33}}{\sqrt{3}} - K\right) \end{cases} \quad (43)$$

## 4. Model Validation and Analysis

### *4.1. Triaxial Creep Model Validation*

The fractional triaxial creep model proposed in this paper considers the influence of thermo-mechanical coupling damage. To validate the model, coal creep experimental data under different temperature and stress conditions are utilized, and model parameters are determined. Zhang et al. [36] conducted creep experiments on coal samples under various temperature and stress conditions, analyzing the mechanisms of temperature and stress on coal creep. In this study, the creep experimental data for the coal sample UCT-3 from their experiments are selected to validate the proposed model. It is known that the stress and temperature conditions for this creep test are axial stress of 30 MPa, confining pressure of 5 MPa, and a temperature of 70 °C.

As depicted in Figure 6, the results obtained from the fractional triaxial creep model show a strong correlation with the experimental curve, particularly evident during the tertiary creep stage. This underscores the effectiveness of the creep model in capturing the entire process of coal creep. It substantiates the importance of accounting for the influence of thermo-mechanical coupling damage when developing a creep model, especially in elucidating the underlying mechanism behind the significant increase in deformation after yielding. Through fitting, the mechanical parameters of the fractional triaxial model were determined, as outlined in Table 1.

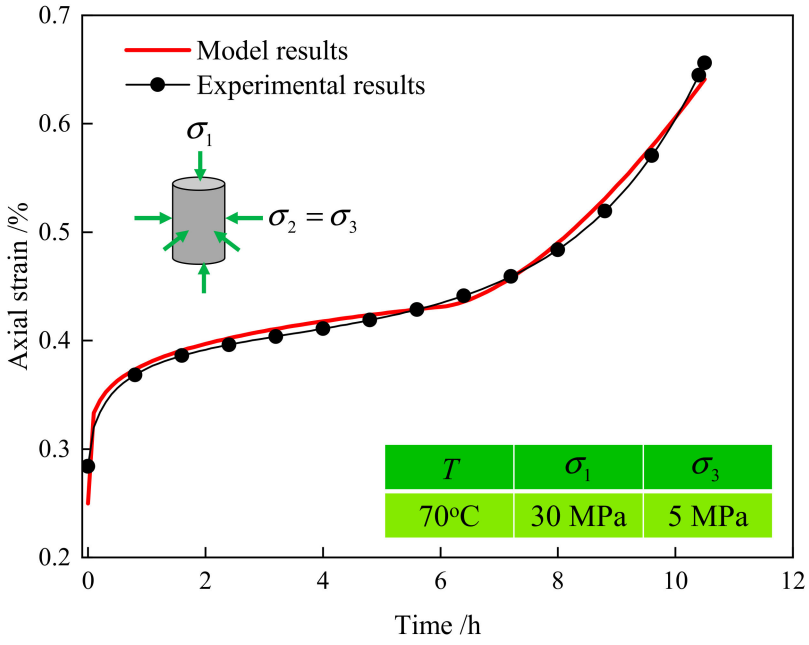


**Figure 6.** Comparative analysis of creep model results and experimental data at 70 °C.

**Table 1.** Mechanical parameters and magnitudes.

| Parameter | Value | Parameter | Value |
|---|---|---|---|
| Shear modulus ($G_M$, GPa) | 6.50 | Thermal expansion coefficient ($\alpha_T$, $K^{-1}$) | $1.0 \times 10^{-4}$ |
| Bulk modulus ($K_M$, GPa) | 5.50 | Temperature effect constant (a) | $-1.0 \times 10^{-3}$ |
| Viscosity coefficient ($\eta_M^{\gamma_1}$, GPa·h$^{\gamma 1}$) | 34.00 | Temperature effect constant (b) | 0.03 |
| Viscosity coefficient ($\eta_{vp}^{\gamma_2}$, GPa·h$^{\gamma 2}$) | 45.00 | Time effect constant ($\omega$, $h^{-1}$) | $1.0 \times 10^{-4}$ |
| Conformable derivative order ($\gamma_1$) | 0.19 | Cohesion ($c$, MPa) | 1.50 |
| Conformable derivative order($\gamma_2$) | 0.94 | Internal friction angle ($\varphi$, °) | 35.56 |

To thoroughly validate the applicability of the fractional triaxial creep model under different temperature and stress conditions, we continue to select different sets of creep experimental data for model validation. Zhou et al. [38] conducted creep experiments on coal samples at temperatures of 200 °C and 400 °C. For the coal sample tested at 200 °C, the axial stress was 15.6 MPa, and the confining pressure was 10.4 MPa. The creep period for this sample lasted up to 106 h, during which only the two creep stages were observed, without entering the accelerated creep stage. For the coal sample tested at 400 °C, the axial stress was 13.0 MPa, and the confining pressure was 8.7 MPa. Although the stress level was relatively low for this sample, it entered the accelerated creep process within a relatively short period. The reason behind this phenomenon is attributed to the higher temperature exacerbating damage accumulation in the coal sample. The specific evolution trends are illustrated in Figures 7 and 8.

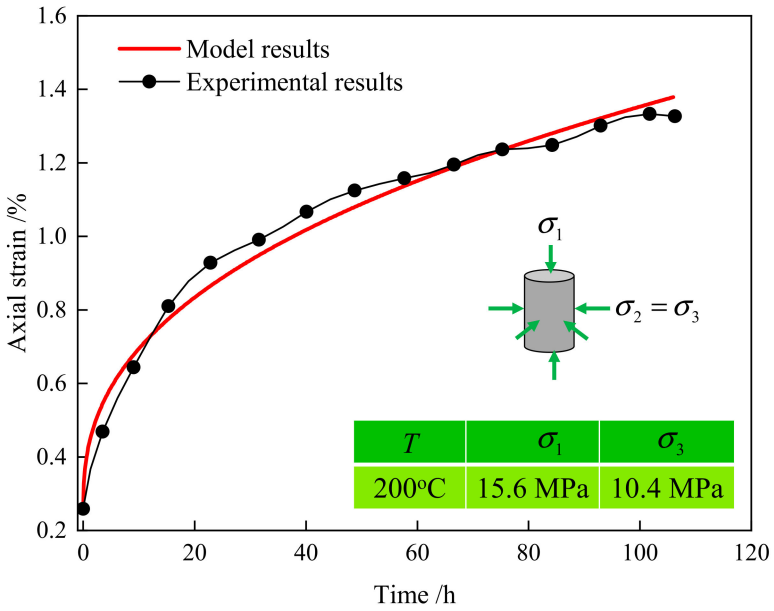


**Figure 7.** Comparative analysis of creep model results and experimental data at 200 °C.

The creep experimental data mentioned above have been selected to validate the proposed creep model. Through comparative analysis between the model results and the creep data, it is observed that the creep process of the coal samples tested at temperatures of 200 °C and 400 °C, particularly the accelerated creep process under high-temperature conditions, is accurately described by the creep model. It is noteworthy that although the external load on the coal sample tested at 400 °C was relatively low, the magnitude of creep deformation for this sample was much greater than that of the coal sample tested at 200 °C. This phenomenon can be attributed to the exacerbation of internal damage within the coal sample due to the high temperature, resulting in a weakened resistance to deformation and degradation of mechanical parameters, leading to significant creep deformation. The

degradation of mechanical parameters due to exacerbated damage is also confirmed by the mechanical parameter values of the creep model under different temperatures in Table 2.

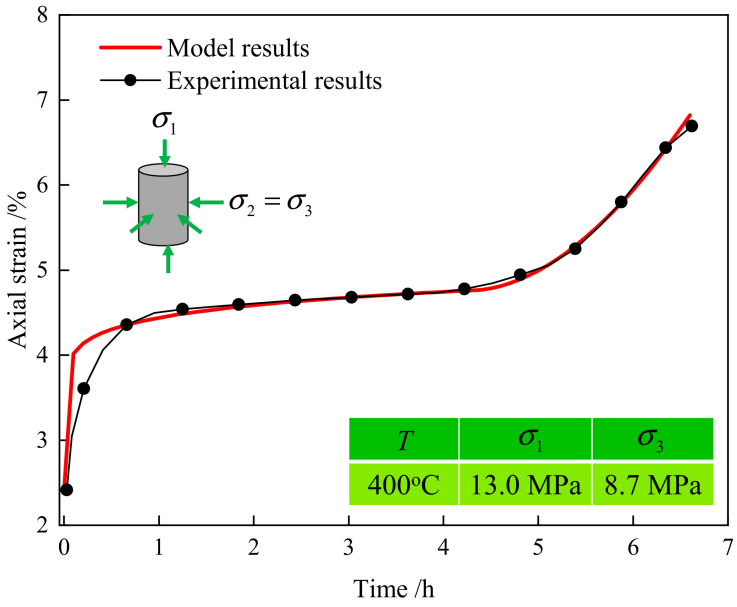


**Figure 8.** Comparative analysis of creep model results and experimental data at 400 °C.

**Table 2.** Mechanical parameters and magnitudes for creep tests.

| Temperature/°C | $G_M$/GPa | $K_M$/GPa | $\eta_M^{\gamma_1}$/GPa·h$^{\gamma 1}$ | $\eta_{vp}^{\gamma_2}$/GPa·h$^{\gamma 2}$ | $\gamma_1$ | $\gamma_2$ |
|---|---|---|---|---|---|---|
| 200 | 6.49 | 5.51 | 2.50 | 45.00 | 0.40 | 0.94 |
| 400 | 0.80 | 1.00 | 0.70 | 3.10 | 0.10 | 0.92 |

### *4.2. Analysis of the Influence Mechanism of Creep Deformation*

Based on the validated applicability and accuracy of the fractional triaxial creep model, an analysis of the influence mechanism of key parameters in the model is now conducted to further clarify the creep deformation under different parameter values.

The influence of different stress levels on creep deformation is analyzed with the model parameters in Table 1. Under a temperature of 70 °C and a confining pressure of 5 MPa, the axial stresses are set at 30 MPa, 40 MPa, and 50 MPa, respectively. According to the axial strain curves in Figure 9, it can be observed that higher axial stress leads to greater axial creep deformation, and the tertiary creep stage of the coal sample occurs earlier. The evolution trend of the model indicates that higher axial stress is more likely to induce accelerated creep, which aligns with the actual deformation evolution trend of coal samples. This further confirms the effectiveness of the proposed creep model.

In order to study the creep deformation of coal under different temperature conditions, an analysis is conducted using Equation (43), and the creep temperatures are set to 50 °C, 70 °C, and 90 °C, respectively. As shown in Figure 10, higher temperatures result in greater creep deformation under an axial pressure of 30 MPa and a confining pressure of 5 MPa. The instantaneous deformation and creep deformation increase with rising temperature, leading to a corresponding increase in the total deformation of the coal sample. These results demonstrate that using thermo-mechanical equivalent stress to establish coupling damage variables and introducing coupling damage variables into the conformable derivative order is feasible. It also reflects the weakening of the mechanical parameters of the coal sample caused by high temperatures, resulting in a gradual increase in creep deformation.

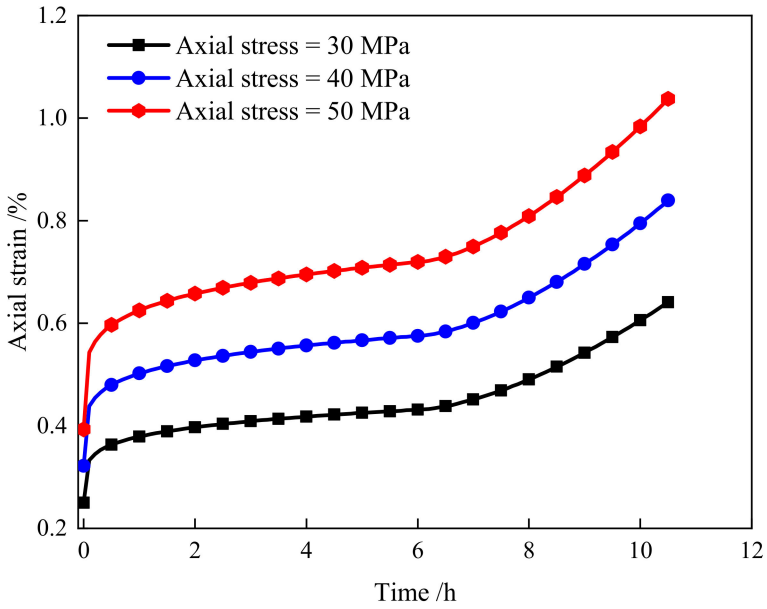


**Figure 9.** Creep strain curves with different axial stress levels.

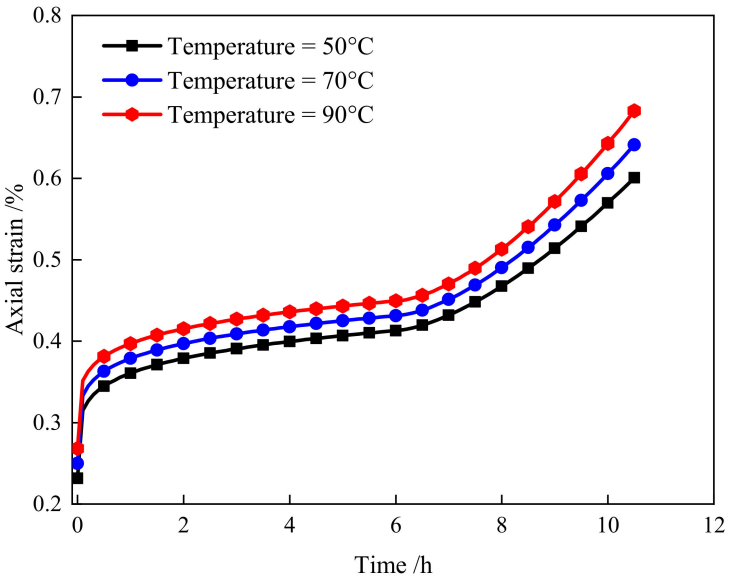


**Figure 10.** Creep strain curves with different temperatures.

The fractional triaxial creep model proposed in this study differs from the traditional Burgers model, and it not only considers the influence of thermo-mechanical coupling damage but also employs conformable derivatives to investigate creep problems. Combining the same model parameters, the conformable derivative order values corresponding to the damaged Abel dashpot are set to 0.8, 0.9, and 1.0, respectively, and the effect of the conformable derivative order on the creep deformation is analyzed. As shown in Figure 11, when the axial pressure, confining pressure, and temperature are 30 MPa, 5 MPa, and 70 °C, respectively, a higher conformable derivative order results in larger creep deformation during the accelerated creep stage. Additionally, with longer creep times, the differences in creep deformation corresponding to different orders become more significant. The evolution trend demonstrates that conformable derivative order has good flexibility in describing nonlinear creep behavior, particularly as the variation in the conformable derivative order directly influences the sudden increase in creep deformation during the accelerated creep stage.

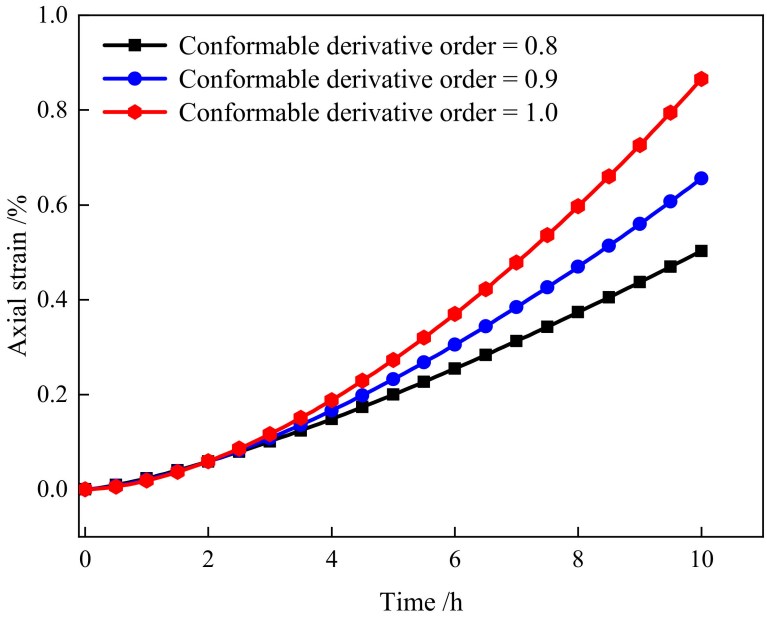


**Figure 11.** Creep strain curves with different conformable derivative orders.

## 5. Conclusions

To study the creep deformation of coal under high temperature and high geostress conditions, a fractional triaxial creep model that accounts for the thermo-mechanical coupling damage effect is established in this study, and the following key conclusions are drawn:

(1) The damaged Abel dashpot and thermo-mechanical coupling damage variable are defined based on the conformable derivative and the Weibull distribution, respectively. A thermo-mechanical coupling damage Abel dashpot is constructed, and this new dashpot component is incorporated into the traditional Burgers model. Considering the triaxial stress state of deep coal, a fractional triaxial creep model for deep coal considering thermo-mechanical coupling damage is established.

(2) The proposed creep model is validated using creep data obtained from coal samples subjected to different temperature and stress conditions. Model parameters are determined by fitting experimental data. Through the fitting analysis, it is observed that the model could effectively describe the time-dependent deformation of coal samples under various temperature and stress conditions, particularly during the accelerated creep stage. It uncovers the intrinsic mechanism wherein high temperatures exacerbate internal damage in coal samples, weaken their resistance to deformation, and result in significant creep deformation.

(3) Based on the analysis of the influence mechanism of key parameters, it is found that higher axial stress levels lead to larger axial creep deformation under identical creep time conditions, and the accelerated creep stage of coal samples occurs earlier. A higher order of conformable derivative results in greater creep deformation during the accelerated creep stage. At the same external stress, both instantaneous and creep deformations of coal samples increase with rising temperatures, thereby leading to a larger total deformation of coal samples as the temperature increases.

**Author Contributions:** Conceptualization, L.Z. and W.J.; Methodology, K.H.; Validation, C.Z.; Formal analysis, S.X.; Investigation, W.J. and L.S.; Writing—original draft, L.Z.; Writing—review & editing, C.Z. All authors have read and agreed to the published version of the manuscript.

**Funding:** The authors are very grateful for the financial support from the China Postdoctoral Science Foundation (2022M722346), the Natural Science Foundation of Shanxi Province (202303021212073, 202303021212217).

**Data Availability Statement:** The original contributions presented in the study are included in the article, further inquiries can be directed to the corresponding authors.

**Acknowledgments:** The authors wish to thank the reviewers and the editor for their kind advice, which has significantly enhanced the soundness of this paper.

**Conflicts of Interest:** The authors declare no conflict of interest.

## References

1. Xie, H.P.; Xie, J.; Gao, M.Z.; Zhang, R.; Zhou, H.W.; Gao, F.; Zhang, Z.T. Theoretical and experimental validation of mining enhanced permeability for simultaneous exploitation of coal and gas. *Environ. Earth Sci.* **2015**, *73*, 5951–5962. [CrossRef]
2. Noack, K. Control of gas emissions in underground coal mines. *Int. J. Coal Geol.* **1998**, *35*, 57–82. [CrossRef]
3. Schoenball, M.; Sahara, D.P.; Kohl, T. Time-dependent brittle creep as a mechanism for time-delayed wellbore failure. *Int. J. Rock Mech. Min. Sci.* **2014**, *70*, 400–406. [CrossRef]
4. Zhao, Y.; Lin, B.Q.; Liu, T.; Zheng, Y.N.; Kong, J.; Li, Q.Z.; Song, H.R. Flow field evolution during gas depletion considering creep deformation. *J. Nat. Gas Sci. Eng.* **2019**, *65*, 45–55. [CrossRef]
5. Guo, Z.H.; Vu, P.N.H.; Hussain, F. A laboratory study of the effect of creep and fines migration on coal permeability during single-phase flow. *Int. J. Coal Geol.* **2018**, *200*, 61–76. [CrossRef]
6. Danesh, N.N.; Chen, Z.W.; Connell, L.D.; Kizil, M.S.; Pan, Z.J.; Aminossadati, S.M. Characterization of creep in coal and its impact on permeability: An experimental study. *Int. J. Coal Geol.* **2017**, *173*, 200–211. [CrossRef]
7. Danesh, N.N.; Chen, Z.W.; Aminossadati, S.M.; Kizil, M.S.; Pan, Z.J.; Connell, L.D. Impact of creep on the evolution of coal permeability and gas drainage performance. *J. Nat. Gas Sci. Eng.* **2016**, *33*, 469–482. [CrossRef]
8. Zhang, L.; Li, X.C.; Ren, T. A theoretical and experimental study of stress–strain, creep and failure mechanisms of intact coal. *Rock Mech. Rock Eng.* **2020**, *53*, 5641–5658. [CrossRef]
9. Cao, S.G.; Xian, X.F. Testing study on the characteristics of creep and damage of coal and other rocks. *Chin. J. Rock Mech. Eng.* **2001**, *6*, 817–821.
10. Wang, D.K.; Liu, J.; Yin, G.Z.; Wei, X.J. Test study of creep properties of gas-bearing coal specimens under triaxial compression. *Chin. J. Rock Mech. Eng.* **2010**, *29*, 349–357.
11. Wang, W.Z.; Yin, G.Z.; Wang, D.K.; Qin, H. A visco-elasto-plastic creep model of outburst prone coal under triaxial compression. *J. Chongqing Univ.* **2010**, *33*, 99–103.
12. Yin, G.Z.; He, B.; Wang, H.; Zhang, X.M. Damage law of overlying rock induced by mining. *J. China Coal Soc.* **2015**, *40*, 1390–1395.
13. Wang, D.K.; Yin, G.Z.; Zhang, D.M. Triaxial creep model and its stability analysis of gas-containing coal. *J. Chongqing Univ.* **2009**, *32*, 1316–1320.
14. Qi, Y.J.; Jiang, Q.H.; WANG, Z.J.; Zhou, C.B. 3D Creep Constitutive Equation of modified Nishihara Model and Its Parameters Identification. *Chin. J. Rock Mech. Eng.* **2012**, *31*, 347–355.
15. Cai, T.T.; Feng, Z.C.; Zhao, D.; Jiang, Y.L. A creep model for lean coal based on hardening-damage mechanism. *Rock Soil Mech.* **2018**, *39*, 61–68.
16. Qu, L.N. A nonlinear Burgers model based on triaxial creep test of coal. *J. Xi'Univ. Sci. Technol.* **2019**, *39*, 985–991.
17. Wu, F.; Chen, J.; Zou, Q.L. A nonlinear creep damage model for salt rock. *Int. J. Damage Mech.* **2019**, *28*, 758–771. [CrossRef]
18. Zhou, F.X.; Wang, L.Y.; Liu, H.B. A fractional elasto-viscoplastic model for describing creep behavior of soft soil. *Acta Geotech.* **2021**, *16*, 67–76. [CrossRef]
19. Zhou, H.W.; Wang, C.P.; Han, B.B.; Duan, Z.Q. A creep constitutive model for salt rock based on fractional derivatives. *Int. J. Rock Mech. Min. Sci.* **2011**, *48*, 116–121. [CrossRef]
20. Kang, J.H.; Zhou, F.B.; Liu, C.; Liu, Y.K. A fractional non-linear creep model for coal considering damage effect and experimental validation. *Int. J. Non-Linear Mech.* **2015**, *76*, 20–28. [CrossRef]
21. Wang, L.J.; Zhou, H.W.; Rong, T.L.; Ren, W.G. Research on experimental and nonlinear creep constitutive model of coal at depth. *J. China Coal Soc.* **2018**, *43*, 2196–2202.
22. Cai, T.T. *Experimental Investigation on the Rheology-Seepage Evolution Law of Coal by Thermal-Mechanical Coupling*; Taiyuan University of Technology: Taiyuan, China, 2018.
23. Xu, T.; Zhou, G.L.; Heap, M.J.; Zhu, W.C.; Chen, C.F.; Baud, P. The influence of temperature on time-dependent deformation and failure in granite: A mesoscale modeling approach. *Rock Mech. Rock Eng.* **2017**, *50*, 2345–2364. [CrossRef]
24. Chen, L.; Wang, C.P.; Liu, J.F.; Liu, Y.M.; Liu, J.; Su, R.; Wang, J. A damage-mechanism-based creep model considering temperature effect in granite. *Mech. Res. Commun.* **2014**, *56*, 76–82. [CrossRef]
25. Zuo, J.P.; Man, K.; Cao, H.; Yang, G.X.; Hu, C.P. Study on Constitutive Equation of Rock Rheological Model with Thermo-Mechanical Coupling Effects. *Chin. J. Rock Mech. Eng.* **2008**, *S1*, 2610–2616.
26. Xi, B.P.; Zhao, Y.S.; Wan, Z.J.; Zhao, J.C.; Wang, Y. Study of Constitutive Equation of Granite Rheological Model with Thermo-Mechanical Coupling Effects. *Chin. J. Rock Mech. Eng.* **2009**, *28*, 956–967.
27. Xu, X.L.; Karakus, M. A coupled thermo-mechanical damage model for granite. *Int. J. Rock Mech. Min. Sci.* **2018**, *103*, 195–204. [CrossRef]

28. Zhang, L.; Zhou, H.W.; Wang, X.Y.; Deng, T.F.; Chen, C.F.; Zhang, H.; Nagel, T. Modeling the visco-elastoplastic behavior of deep coal based on conformable derivative. *Mech. Time-Depend. Mater.* **2023**, 1–21. [CrossRef]
29. Zhou, H.W.; Su, T.; Deng, H.L.; Wang, R.; Zhao, J.W.; Sun, X.T.; An, L. Characterizing three-dimensional creep of Beishan granite by the variable-coefficient Abel dashpot. *Mech. Time-Depend. Mater.* **2021**, *25*, 85–100. [CrossRef]
30. Khalil, R.; Al Horani, M.; Yousef, A.; Sababhehb, M. A new definition of fractional derivative. *J. Comput. Appl. Math.* **2014**, *264*, 65–70. [CrossRef]
31. Wu, F.; Liu, J.F.; Wu, Z.D.; Bian, Y.; Zhou, Z.W. Fractional nonlinear creep constitutive model of salt rock. *Rock Soil Mech.* **2014**, *35*, 162–167.
32. Xue, D.J.; Lu, L.L.; Yi, H.Y.; Wu, Z.D.; Zhang, Q.S.; Zhang, Z.P. A fractional Burgers model for uniaxial and triaxial creep of damaged salt-rock considering temperature and volume-stress. *Chin. J. Rock Mech. Eng.* **2021**, *40*, 315–329.
33. Zhou, H.W.; Jia, W.H.; Xie, S.L.; Su, T.; Zhang, L.; Ma, B.W.; Hou, W. A statistical damage-based fractional creep model for Beishan granite. *Mech. Time-Depend. Mater.* **2022**, *27*, 163–183. [CrossRef]
34. Hu, Q.Z.; Feng, X.T.; Zhou, H. Study of creep model of rock salt with thermal damage considered. *Rock Soil Mech.* **2009**, *30*, 2245–2248.
35. Ding, J.Y.; Zhou, H.W.; Chen, Q.; Liu, D.; Liu, J.F. Characters of rheological damage and constitutive model of salt rock. *Rock Soil Mech.* **2015**, *36*, 769–776.
36. Zhang, L.; Zhou, H.W.; Wang, X.Y.; Wang, L.; Su, T.; Wei, Q.; Deng, T.F. A triaxial creep model for deep coal considering temperature effect based on fractional derivative. *Acta Geotech.* **2021**, *17*, 1739–1751. [CrossRef]
37. Nagel, T.; Minkley, W.; BÖttcher, N.; Naumov, D.; GÖrke, U.J.; Kolditz, O. Implicit numerical integration and consistent linearization of inelastic constitutive models of rock salt. *Comput. Struct.* **2017**, *182*, 87–103. [CrossRef]
38. Zhou, C.B.; Wan, Z.J.; Zhang, Y.; Liu, Y.; Zhang, B. Creep characteristics and constitutive model of gas coal mass under high temperature and triaxial stress. *J. China Coal Soc.* **2012**, *37*, 2020–2025.